Oda *et al. Earth, Planets and Space (2018) 70:165*
https://doi.org/10.1186/s40623-018-0924-3

Earth, Planets and Space

EXPRESS LETTER

Open Access

Characterization of marine ferromanganese crust from the Pacific using residues of selective chemical leaching: identification of fossil magnetotactic bacteria with FE-SEM and rock magnetic methods

Hirokuni Oda[1*], Yoshio Nakasato[2] and Akira Usui[3]

Abstract

Hydrogenetic ferromanganese crusts (hereafter referred to as "crusts") on Pacific seamounts are formed by the precipitation of iron–manganese oxides from seawater on volcanic and biogenic substrate rocks. As crusts grow continuously and have very slow growth rates of between 1 and 10 mm/m.y., they can potentially be used as records of the Neogene paleoceanographic and paleoclimatic conditions. Crusts can be considered as compressed sediment cores containing biogenic, volcanogenic, and terrestrial particles that include eolian dusts and the partly weathered products of substrate acquired during its growth. In this study, selective leaching experiments were conducted on a sample of ferromanganese crust, which had been obtained from the Federated States of Micronesia at a water depth of 2262 m. Chemical leaching experiments were conducted using oxalic acid buffered with ammonium oxalate on the crushed crust samples, which is an optimization of previously proposed sequential leaching procedures. The applied method was found to be effective in separating the major mineral phases of crusts from associated metallic components, thereby providing concentration of the residual fraction for use in analysis following the leaching experiment. Using this method, polygenetic particles were extracted from the crust and identified using optical and electron microscopes. They were found to be of various origins and included volcanogenic, biogenic, terrestrial, and extraterrestrial material. In addition, well-sorted prism-shaped chained magnetic particles were observed in residual fractions. Rock magnetic experiments support the idea that the magnetic particles are magnetites and originated from fossil magnetotactic bacteria. The fossil magnetotactic bacteria might have been living on the crust at the time of crust formation. Alternatively, fossil magnetotactic bacteria could have been transported by deep sea currents from the sediment where magnetotactic bacteria originated.

Keywords: Ferromanganese crust, Magnetotactic bacteria, Terrestrial, Extraterrestrial, Eolian, Cosmic spherule, Titanomagnetite, Chemical leaching, Rock magnetism

*Correspondence: hirokuni-oda@aist.go.jp
[1] Research Institute of Geology and Geoinformation, Geological Survey of Japan, AIST, Central 7, 1-1-1 Higashi, Tsukuba 305-8567, Japan
Full list of author information is available at the end of the article

Introduction

Hydrogenetic ferromanganese crusts (hereafter referred to as "crusts") on Pacific seamounts are formed by precipitation of iron–manganese oxides from seawater on volcanic and biogenic substrate rocks. Crusts grow continuously with very slow growth rates of between 1 and 10 mm/m.y., and they can thus potentially be used as records of the Neogene paleoceanographic and paleoclimatic conditions (e.g., Usui et al. 2007). Chemical compositions of ferromanganese crusts can be obtained through observations with optical and electron microscopes and conducting chemical mapping on a polished surface. However, these methods cannot always provide adequate information, as minor particles are hidden in the matrix, which are mainly composed of vernadite (chemical formula $(Mn^{4+}, Fe^{3+}, Ca, Na)(O,OH)_2 \cdot n(H_2O)$; Anthony et al. 2018), and observation of the surface of large materials, such as fossils, is also limited. With these limitations in mind, this study presents a novel selective dissolution technique that targets vernadite and provides a more direct means for examining the materials preserved within the ferromanganese crusts.

The leaching technique is also important for use in exposing and identifying magnetic minerals hidden in the matrix of crusts and for removing largely paramagnetic components in the matrix that hinder conducting certain rock magnetic measurements. Thin slices of ferromanganese crust have been measured using a SQUID Rock Magnetometer (e.g., Joshima and Usui 1998; Noguchi et al. 2017a; Yuan et al. 2017), which provides submillimeter- to millimeter-scale magnetostratigraphy, and a scanning SQUID microscope (e.g., Oda et al. 2011; Noguchi et al. 2017b), thereby providing an alternative dating method of crusts, and results have shown that the crust has stable remanent magnetization. Noguchi et al. (2017b) reported rock magnetic results including magnetic hysteresis properties from a crust in the northwestern Pacific that suggest three phases of magnetic minerals with mean coercivities of associated phases of 18–25 mT, 31–32 mT, and 930–1200 mT, respectively (Supplementary material: Noguchi et al. 2017b). In this study, we applied a leaching method to extract and report magnetite particles that are assumed to have originated from magnetotactic bacteria. Rock magnetic experiments were also conducted to confirm the presence of biogenic magnetite, which may correspond to the second phase reported in Noguchi et al. (2017b).

Geological setting, samples, and chemical leaching

A marine ferromanganese crust sample (MC10CB07; Fig. 1c) was taken from the MC10 Seamount (9°45′N, 148°16′E) located close to Micronesia during a Japanese cruise with R/V Hakurei-maru No. 2 in 1997. The survey focused on sea bottom observations using a Finder-installed Deepsea Camera, and sampling was conducted using dredgers. The MC10 Seamount is located at an ocean depth of less than 3000 m, and its flat top rises to a water depth of 2000 m. Twenty crust samples with average thicknesses of 20 mm (three of them are thicker than 100 mm) were collected from the seamount. The largest crust sample MC10CB07 was taken from a saddle of the seamount (marked on Fig. 1b; lat = 9°57.924′N,lon = 148°16.157′E, water depth = 2262 m) at an area north of the summit's flat top. The crust sample MC10CB07 has an average thickness of 110 mm with a maximum thickness of 155 mm, and its substrate is an altered and phosphatized basalt (substrate rock; Fig. 1d).

An age model has already been developed by Nishi et al. (2017) using $^{10}Be/^{9}Be$ methods on the crust sample MC10CB07. The results show a constant growth rate of ~ 2.0 mm/m.y. from 7.7 Ma to the present (Table 2 and Figure 6: Nishi et al. 2017). However, the growth rate from the middle Miocene to 7.7 Ma was 3.5 mm/m.y., and it has been deduced that the rate prior to the middle Miocene was higher than 20 mm/m.y (Nishi et al. 2017).

The crust sample MC10CB07 was divided into three layers based on appearance, optical microscope observations, and mineralogical and chemical compositions (Figs. 1d, 2a, b). The first (0–10 mm from the surface) layer is black and dense and contains wave-like structures; the second layer (~ 70 mm thickness) is black and brown (mixed colors) with columnar structures that include a large amount of detrital grains; and the third layer (~ 50 mm thickness) is a phosphatized, dense, black layer that includes calcareous ooze. Kim et al. (2006) reported similar stratigraphy for crusts taken from the same latitude band. Although it was possible to identify the detrital materials using XRD analysis, chemical leaching technique was applied to extract detrital grains by dissolving ferromanganese oxides that were the main components.

Sample preparations and measurements

Chip samples with thicknesses of 3 mm were prepared from a slab sample of the crust (optical photograph image; Fig. 2a), and 33 chips were measured using an X-ray powder diffractometer (XRD) (RIGAKU MultiFlex) at Kochi University with Cu Kα radiation operated at 40 kV and 16 mA at a speed of 8°/min. X-ray fluorescence (XRF) analyses of another slab sample (optical photograph image; Fig. 2b) of the crust were also conducted using a micro-XRF analyzer (HORIBA XGT-7200 V) at Kochi University operated at 50 kV and 1 A with 100 μm beam diameter.

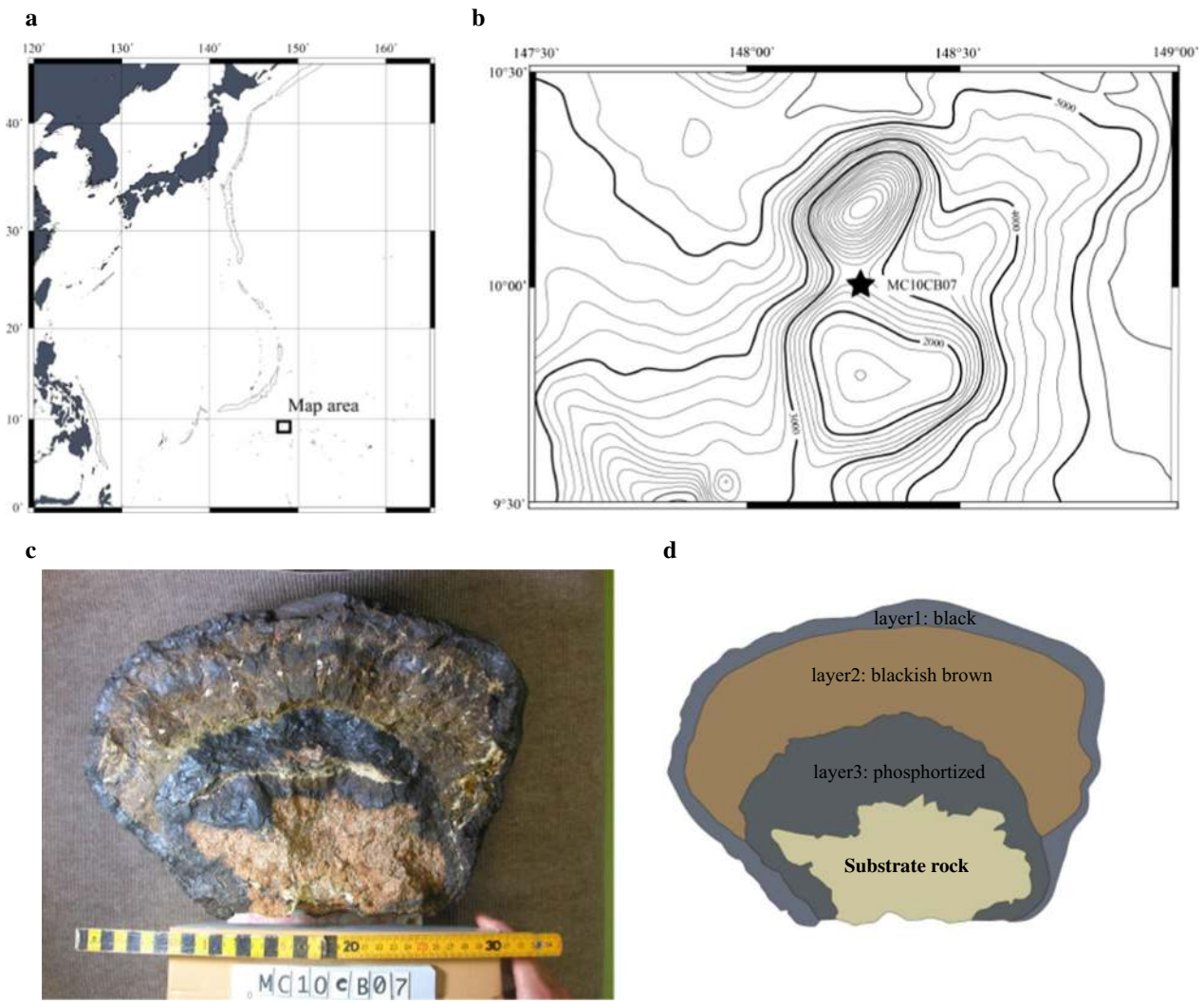

Fig. 1 Sampling sites, crust sample, and depth profiles used in chemical analysis. **a** Index map showing area of study around Micronesia in the northwestern Pacific. **b** Local map showing sampling site and bathymetry of area. **c** Photograph of crust sample MC10CB07 and **d** layers identified using naked eye observation that was primarily based on colors

We applied a chemical leaching method for extracting detrital grains contained in the crust. To remove the main matrix material vernadite, we used basically the third part of the sequential chemical leaching method proposed by Koschinsky and Halbach (1995). The method is to employ oxalic acid buffered with ammonium oxalate (pH 3.0; 100 mL) on the crust sample (0.5 g) crushed down to < 300 μm. The mixture was stirred at 25 °C, and sieved while washing with distilled water. Experiments were conducted on materials obtained from the first and second layers but excluded materials from the third layer as these had been phosphatized. The sampling and chemical leaching experiments were conducted on four units that were classified based on visual observations, optical microscopy, and XRD analysis (Fig. 2c).

The remaining materials (e.g., Fig. 3 and Additional file 2: Fig. S2) were sieved and then described using observations made with optical and electron microscopes. Observations of secondary electron images were made using a FE-SEM JSM–7001F (Nihon-Denshi Co. Ltd.) at Kochi University, and chemical analyses were also made with an equipped energy-dispersive X-ray spectroscopy (EDS) for grains larger than ~ 10 μm.

Rock magnetic measurements were conducted to characterize magnetic minerals contained in the crust. A fragment of a sample was taken from the upper part of Unit 1 (0–10 mm; Sample 1) where possible magnetotactic bacteria were found (see next section) and divided into three for the following rock magnetic experiments. High-temperature susceptibility was measured in air

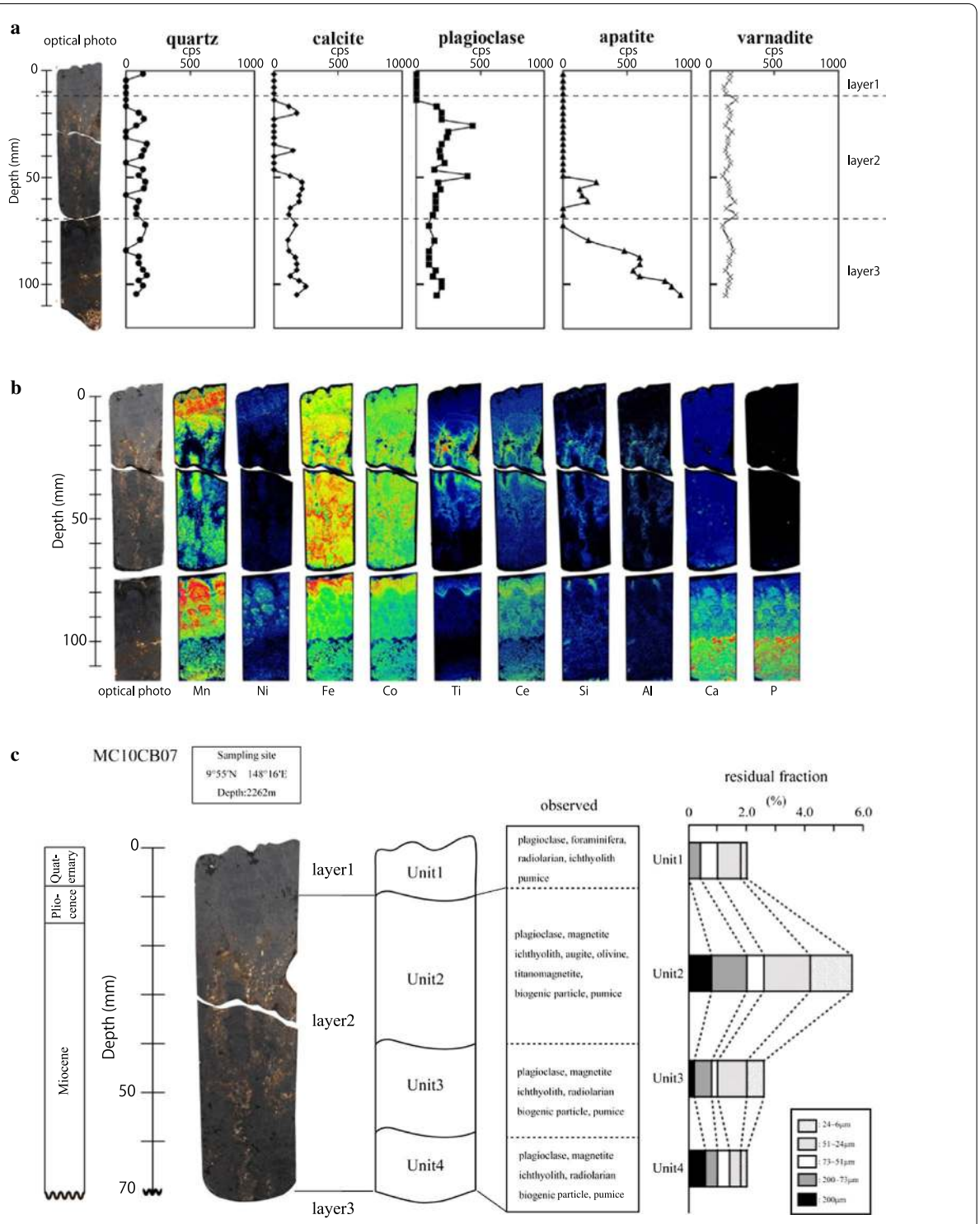

Fig. 2 **a** Results of XRD analyses measured on ~ 3 mm chip taken from polished section shown as photographic images on the left. Horizontal scale for each mineral show count per second (cps) value for a characteristic peak of each mineral. **b** Distribution of Mn, Ni, and Fe (from left to right) based on XRF analysis on another polished section shown as photographic images on the left. **c** Diagrams summarizing chemical leaching experiments. From left to right, age model based on ^{10}Be chronology, photograph of a polished section, units classified based on visual observations, optical microscopy and XRD analysis, observed materials within the residue, and fractions of each size within the residues. Observations for Fig. 3c were conducted using the material on 6-μm mesh sieve. 'Biogenic particles' in the observed materials column represents unidentified partially dissolved apatite particles considered to be originated from fossils. Residual fraction shows weight percentage of each size fraction obtained after chemical leaching of starting material (0.5 g)

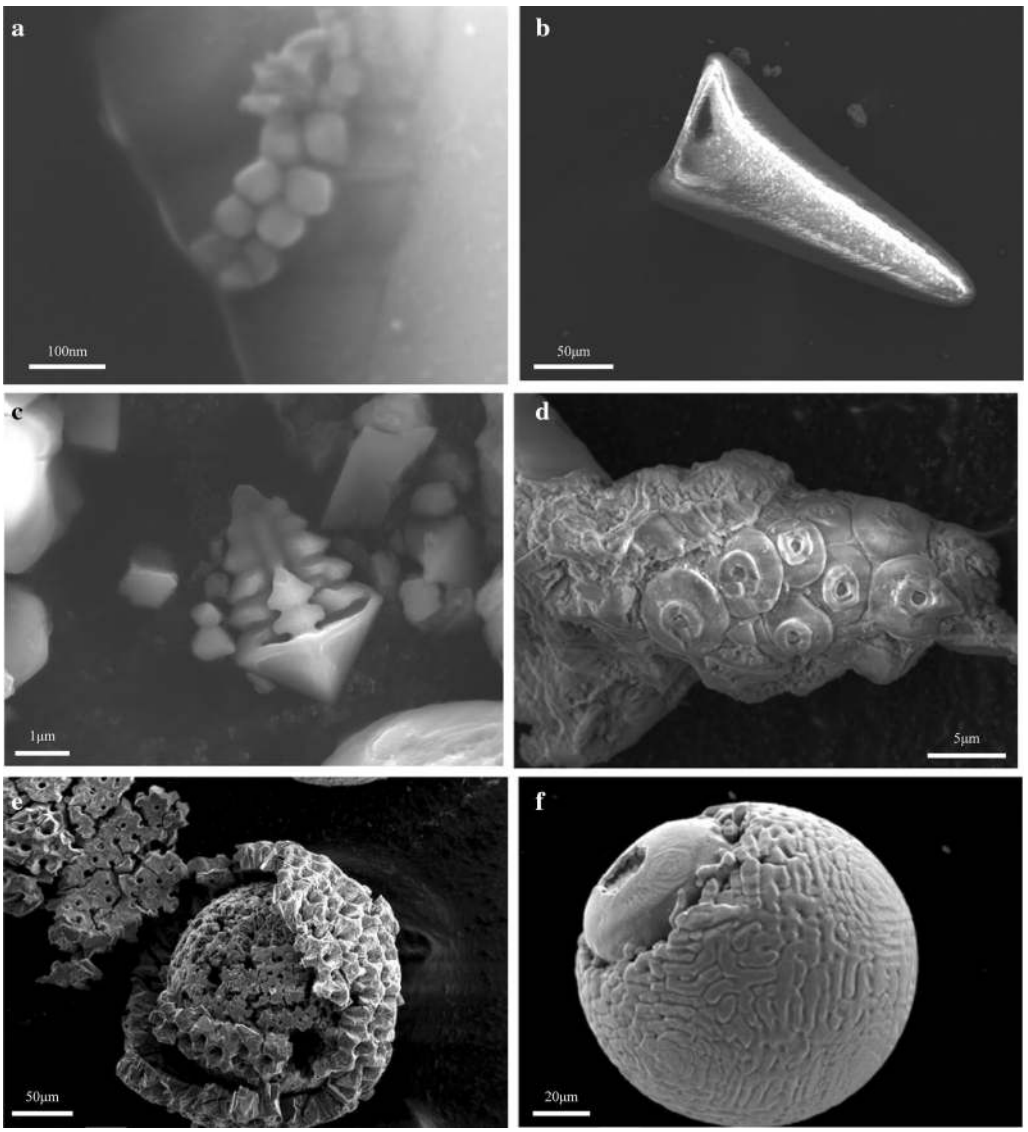

Fig. 3 Secondary electron images of extracted materials observed with FE-SEM; **a** chain of magnetic particles considered to be fossil biogenic magnetite, **b** icthyolith, **c** titanomagnetite with dendritic texture, **d** coccolith, **e** foraminifera, and **f** cosmic spherule. **a**–**c**, **f** are observed with 15 kV, whereas **d**, **e** were observed with 5 kV. Particles in **a** were extracted from Unit 1, and others from Unit 2. The identification of the origin of the grains was primarily based on morphologies with the help of chemical analyses using EDS for grains larger than ~ 10 μm

using a Kappabridge KLY-4S (AGICO Co. Ltd.) with high-temperature furnace (CS-3) up to 700 °C with a heating rate of 10 °C/min. Thermal demagnetization experiment was conducted after imparting Isothermal Remanent Magnetization (IRM) at 2.5 T, 0.3 T, and 0.1 T in *X*-, *Y*-, and *Z*- directions in sequence, according to the method proposed by Lowrie (1990). Furthermore, an alternating Gradient Field Magnetometer (Micromag 2900 AGM; Lake Shore Cryotronics, Inc.) was used to conduct magnetic hysteresis experiments, FORC (First Order Reversal Curve) measurements and backfield application to saturation IRM (1.4 T). Analyses of FORC data were conducted using FORCinel software (Harrison and Feinberg 2008) and employed VARIFORC functions for smoothing (Egli 2013). Backfield curves were analyzed using MAX Unmix software (Maxbauer et al. 2016) after subtracting each value from the saturation IRM and dividing by two.

Results

XRD analyzes of chip samples showed the presence of quartz, plagioclase, calcite, apatite and vernadite (Fig. 2a). Vernadite, an iron–manganese oxide mineral, was found

in all three layers, which indicates that the crust is hydrogenetic in origin. Quartz and plagioclase were found mostly in the second layer, calcite was found mostly in the third layer, and apatite was found in the third layer and at the bottom of the second layer.

A map of the elements measured by XRF (Fig. 2b) suggests the following features. There were no elements of detrital origin, such as Si, Al, and Ti, detected in the first layer. There was a significant occurrence of Mn and Ni in the first layer compared to the second layer. The second layer contained more elements of detrital origin (Si, Al, and Ti) but less Mn, which can be interpreted as being the dilution effect by the detrital materials, and the higher amounts of Fe in the first layer are also consistent with this. The third layer had higher amounts of P and Ca, which is consistent with phosphatization of the layer.

The residues of chemical leaching were found to be composed of various kinds of terrestrial and extraterrestrial materials, such as augite, olivine, magnetite, microfossils, cosmic spherules, and eolian dusts (Additional file 1: Fig. S1). It was difficult to identify these in chip samples using XRD analysis. The larger-sized grains (> 24 μm) were not rounded suggesting a proximal origin. These materials are considered to have a volcanogenic origin relating to weathering, erosion, and transportation from surrounding seamounts, and are very rare in Unit 1 but rich in Unit 2.

The slight presence of phosphatization observed with XRD at the boundary between Unit 3 and Unit 4 could be interpreted as being related to an increase in biogenic materials. Biogenic materials are rich in Units 3 and 4 but poor in Units 1 and 2, which indicates that Units 3 and 4 were formed when biogenic productivity was high at the time of corresponding crust formation.

To facilitate observation of small-sized and/or rare magnetic particles, magnetic concentration was conducted for residues taken from Unit 1 (0–10 mm) using a Sm–Co hand magnet. The magnetic concentration was conducted only for Unit 1, because the sample is black and dense, and fraction of small grain size (< 6 μm) is most abundant. The residues were diluted with a distilled water, and dispersed using a stirrer. The hand magnet was put on a plastic tray and gently moved in the container to attract magnetic particles beneath the tray. The tray was lifted up together with the magnet, the bottom surface of the tray was washed in another container with a distilled water after removing the magnet. The process was repeated many times, and the material was collected after evaporating water. For Units 1 through 4, magnetite grains with grain sizes of hundreds of micro-meters to several tens of nano-meters were observed. It was remarkable to find the presence of chains of prism-shaped, uniformly sized, magnetic particles measuring several tens of nano-meters, which are considered to be magnetosomes originating from magnetotactic bacteria (Fig. 3a). Grains presumed to be titanomagnetites (Fig. 3c) and cosmic spherules (Fig. 3f) were also found in the crust. In order to understand the origin of these particles, further study is needed (e.g., presence of Ni for cosmic spherules).

Discussion

Contribution of chemical leaching to paleoenvironment studies

Kim et al. (2006) interpreted the difference between layers 1 and 2 (recognized in crusts taken from a latitudinal band similar to the studied crust MC10CF07) as being related to the position of the ITCZ (Intertropical Convergence Zone). Although Hein et al. (1993) also observed layer 1 and layer 2 in crusts from the northwestern Pacific, they suggested that the difference was not related to the ITCZ. Use of oxalic acid prevents dissolution of calcium carbonate and also enables the extraction of foraminifera, coccoliths, and icthyoliths. Chemical leaching that dissolved the matrix material vernadite enabled us to identify details of the depositional environment recorded by the crust, which would not have been possible if chemical leaching had not been used on bulk samples. The leaching method also enabled us to conduct a detailed biostratigraphy and Sr chronology for crusts using icthyolith (e.g., Gleason et al. 2002).

Paleolatitude of sites

van Hinsbergen et al. (2015) provided a tool for paleoclimate studies to backtrack the paleolatitude into the past for any location on the globe. Paleolatitudes of the site using the software are calculated as 11.3 ± 1.9°N, 10.4 ± 1.8°N, and 10.8 ± 2.6°N for 0, 10, and 20 Ma, respectively. These paleolatitude estimates may not be reliable because these are transferred from the paleolatitudes of the continents through plate circuit assuming that the hotspots are not moving. However, hotspot motion has now been recognized (e.g., Tarduno et al. 2003). Although reliable paleolatitudes of the Pacific could be obtained from volcanic rocks, exposed volcanic rocks are limited. On the other hand, the paleolatitudes obtained from the sediment suffers from inclination shallowing (e.g., Tarduno 1990). Thus, further work is needed on reliable estimates of the Pacific paleolatitudes.

Identification of magnetites formed by magnetotactic bacteria

Magnetic particles formed by magnetotactic bacteria are composed of magnetite (Fe_3O_4) or greigite (Fe_3S_4) crystals ranging in size between ~ 20 nm and ~ 100 nm (e.g., Bazylinski et al. 1994; Yamagishi et al. 2016) and have characteristic morphologies that are cuboctahedra-shaped, elongated prism-shaped, or bullet-shaped, which would have been difficult to form via simple inorganic reactions (e.g., Chang et al. 2014; Yamagishi et al. 2016). One of the morphologies found in the magnetic extracts of the crust in this study (Fig. 3a) is prism-shaped and is considered equivalent to those formed in living magnetotactic bacteria cells. Living magnetotactic bacteria are generally found in ponds, rivers, and oceans. Although fossil magnetotactic bacteria have previously been observed in sediment cores in oceans and lakes (e.g., Lin et al. 2017), this is the first report of magnetotactic bacteria from a marine ferromanganese crust.

To support the idea that the chained magnetic particles originated from fossil magnetotactic bacteria, further investigations were conducted using high-temperature magnetic susceptibility measurements, thermal demagnetization of orthogonal IRM, and magnetic hysteresis analyses (hysteresis loops, DC demagnetization of saturation IRM and FORC analyses). High-temperature susceptibility of a bulk sample from the crust (0–10 mm from the surface) is shown in Fig. 4a. The heating curve shows a significant drop at ~ 570 °C (minimum in the derivative curve; Fig. 4a upper diagram), which suggests the Curie temperature of magnetite. Thermal demagnetization of orthogonal IRM shows a sharp and significant drop at 500 °C and diminishes between 500 and 600 °C in the low coercivity component (0–0.1 T; blue symbol in Fig. 4b), which suggests the existence of nearly stoichiometric magnetite. A slight reduction in the component of 0.1T could be recognized between 250 and 300 °C which might be associated with the unblocking temperature of titanomagnetite found in the residues (Additional file 2: Fig. S2). Higher-coercivity components (0.1–0.3 T: red symbol, 0.3–2.5 T: purple symbol; Fig. 4b) are not obvious and gradually decrease to become almost zero at temperatures lower than 500 °C. Components higher than 600 °C suggesting the clear indication of hematite were not observed in all three components.

The raw magnetic hysteresis curve for the bulk sample (Fig. 5a) shows a large contribution from a paramagnetic component, which may originate from the matrix material vernadite. However, after chemical leaching and extraction of magnetic materials with the Sm–Co hand magnet, the paramagnetic component in the raw

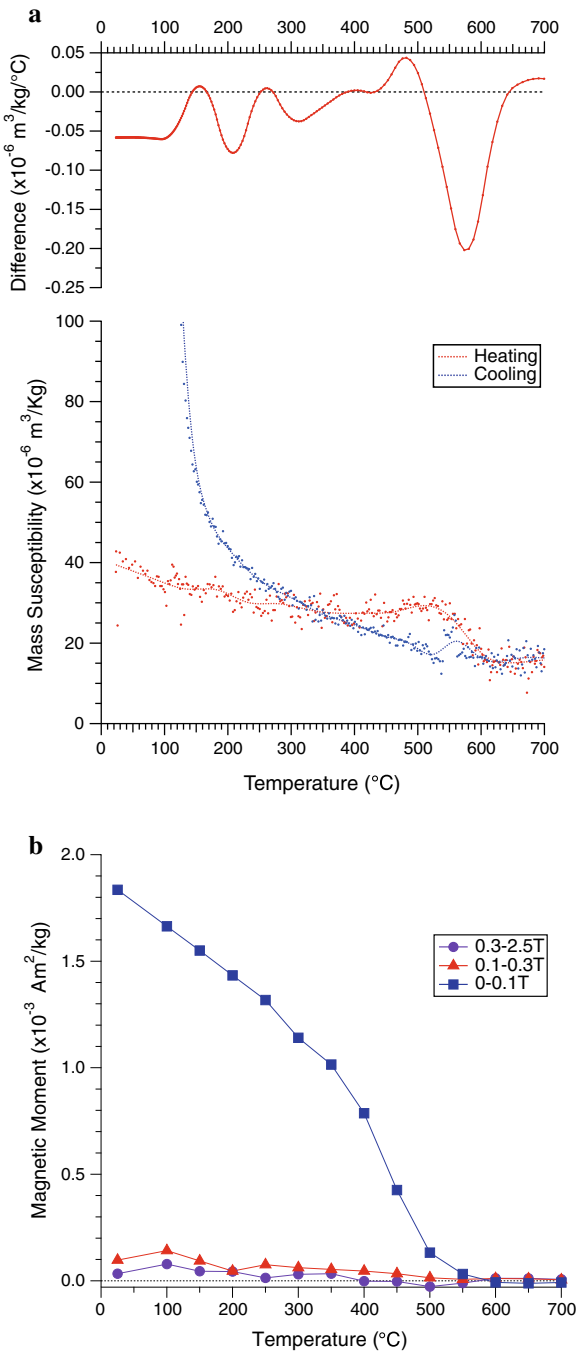

Fig. 4 **a** High-temperature susceptibility (lower diagram) of bulk sample (157.5 mg) for Unit 1 (0–10 mm from surface) representing heating (red dots) and cooling (blue dots) with spline smoothed curves (red and blue curves are for heating and cooling, respectively) with a derivative of the heating curve indicating a sharp drop at 573 °C (upper diagram). **b** Thermal demagnetization of orthogonal IRM based on Lowrie (1990) for a chip sample (20.4 mg) taken from Unit 1 (0–10 mm from surface). *X* (0.3–2.5 T), *Y* (0.1–0.3 T), and *Z* (0–0.1 T) axes are shown in purple, red, and blue, respectively

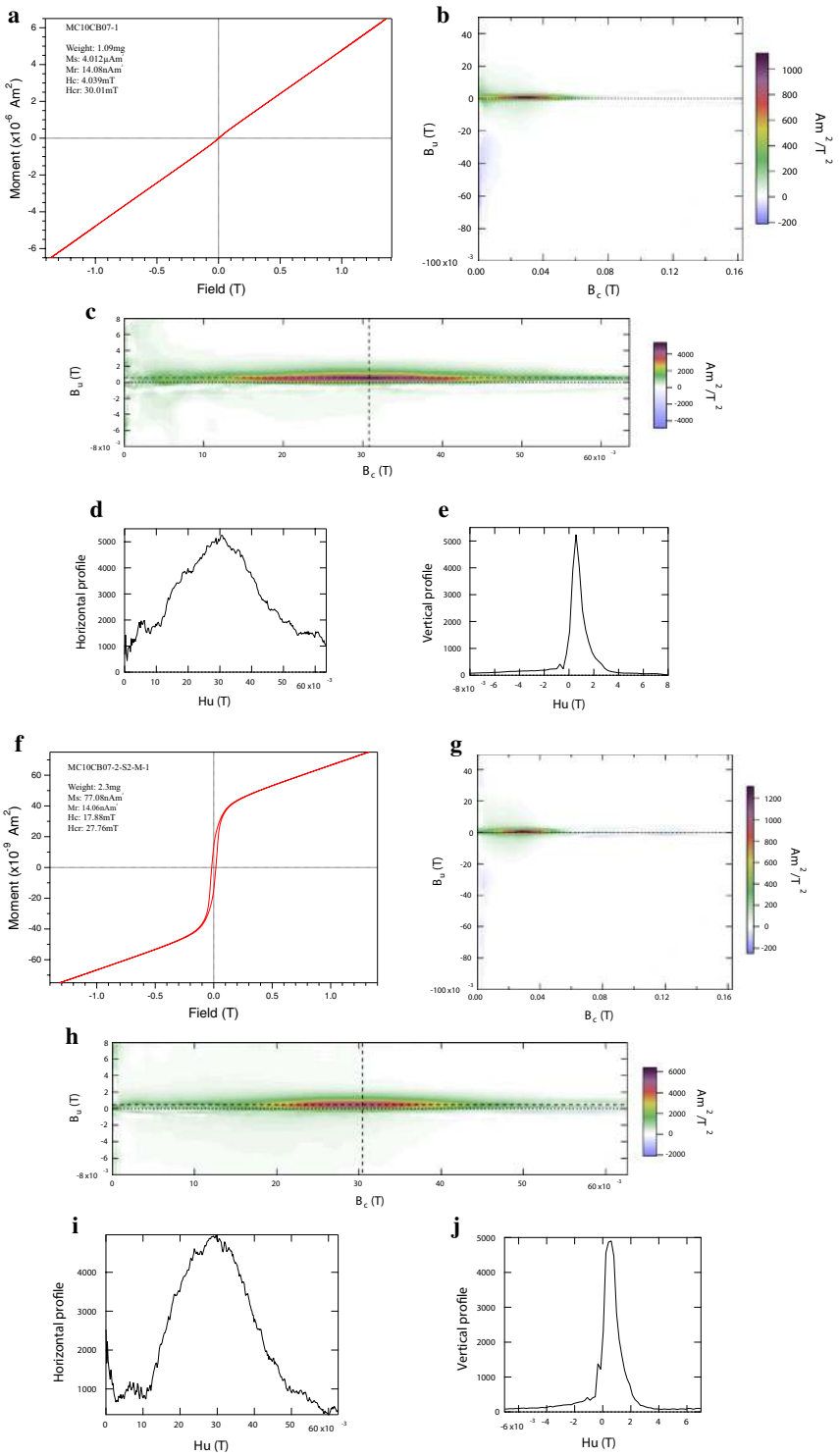

Fig. 5 **a** Hysteresis loops and parameters for a bulk sample (10.9 mg) taken at 0–10 mm from the surface. **b** FORC diagram for the same sample (Bu = − 40 mT ~ + 40 mT, Bc = 0 ~ 150 mT, average time = 100 ms). **c** A closed-up of FORC diagram along the central ridge (Bu = − 5 ~ + 5 mT, Bc = 0 ~ 60 mT, average time = 100 ms) and cross sections **d** along horizontal line at Bu = 0.5 mT and **e** along vertical line at Bu = 31 mT. **f** Hysteresis loops and parameters for the residue after chemical leaching and magnetic extraction (2.3 mg) for a sample taken at 0–10 mm from the surface. **g** FORC diagram for the same sample (Bu = − 40 mT ~ + 40 mT, Bc = 0 ~ 150 mT, averaging time = 100 ms). **h** A closed-up of FORC diagram along the central ridge (Bu = − 5 ~ + 5 mT, Bc = 0 ~ 60 mT, average time = 200 ms) and cross sections **i** along horizontal line at Bu = 0.5 mT and **j** along vertical line at Bu = 33 mT

magnetic hysteresis curve was significantly reduced (Fig. 5f). FORC analysis of a bulk sample showed the presence of a central ridge as a prominent feature (Fig. 5b, c), which is representative of uniaxial, non-interacting, single-domain switching units that are considered to be interacting particles aligned in chains (e.g., Kind et al. 2011) and are typical of biogenic magnetite origin (e.g., Roberts et al. 2014). The median coercivity of the ridge for the sample was measured as 31 mT (Fig. 5d). The horizontal centerline along the central ridge is slightly offset to positive (+0.5 mT), and the vertical cross section at the peak value (31 mT; Fig. 5e) shows clear and sharp features of the central ridge. In addition, the negative region along the vertical axis (Fig. 5b) corresponds to a single-domain behavior (e.g., Roberts et al. 2014). Although hysteresis loop for the material left after magnetic extraction shows negative slope, FORC diagram still indicates the presence of the central ridge (Additional file 3: Fig. S3).

Analyses of backfield curves of three sister samples used for FORC measurements show similar components (Additional file 4: Fig. S4). Major contribution is component 3 with mean coercivity (Bh) of 32–36 mT and narrow dispersion parameter (DP) of 1.4–1.5 mT. Component 4 has Bh = 100–110 mT, which is much smaller compared with the highest coercivity (930–1200 mT) reported by Noguchi et al. (2017b). This may suggest much more eolian input for the site (latitude ~ 22°N) of Noguchi et al. (2017b) than for the studied site (latitude ~ 10°N).

The presence of non-interacting, single-domain magnetite originating from magnetotactic bacteria supports previous evidence that submillimeter-scale magnetostratigraphies can be successfully created using stable remanent magnetization (e.g., Joshima and Usui 1998; Oda et al. 2011; Noguchi et al. 2017a, b; Yuan et al. 2017). Although the question as to why and how magnetotactic bacteria exist in the crust has not been answered, it is possible to assume that magnetotactic bacteria died, were captured by the matrix, and were then locked-in the crust within the magnetic field direction over a reasonably short geological time period, which thus enables their determination by magnetostratigraphy. However, it is important to consider the environmental conditions enabling magnetotactic bacteria to survive on the surface of crust. Therefore, an alternative explanation could be that the magnetotactic bacteria were transported from the deep sea by deep sea currents after death or while living and then deposited together with the matrix.

Conclusions

The study demonstrated a new method for extracting minerals from ferromanganese crusts, which otherwise would be buried and hidden within the vernadite matrix. A selective chemical leaching method that prevented dissolution of calcium carbonate was applied on a crust sample MC10CB07 from the MC10 Seamount near Micronesia. The leaching method enables identification of various materials/particles that provide rich information and the opportunity to understand details of environmental history recorded in the crust. The leaching process was also effective in revealing magnetic minerals and enabled the discovery of chained magnetite grains, which are considered to be from fossil magnetotactic bacteria. The presence of magnetite and uniaxial, non-interacting, single-domain, magnetic particles supports the hypothesis that these are fossil magnetotactic bacteria. Alghouth it remains unclear how the fossil magnetotactic bacteria were incorporated into the materials in the crust, it is considered that they could have been formed on the crust or transported from the deep sea sediments via deep sea currents.

Additional files

Additional File 1: Figure S1. Position of materials extracted from the crust for use in chemical leaching and extraction experiments. (Left) Photographic image of the crust with a rectangle frame indicating the material used for chemical leaching experiments. (Middle) Schematic diagram showing units identified with the rectangle frame. (Right) Minerals identified as XRD counts.

Additional File 2: Figure S2. Examples of optical photographs taken of extracted materials; (a) ilmenite, (b) olivine, (c) plagioclase, (d) icthyolith, (e) augite, (f) magnetite.

Additional File 3: Figure S3. (a) Hysteresis loops and parameters for the material left after magnetic extraction experiments on the residue (3.5 mg). (b) FORC diagram for the same sample (Bu = − 40 mT ~ + 40 mT, Bc = 0 ~ 150 mT, average time = 200 msec, average of two measurements). (c) A closed-up of FORC diagram along the central ridge (Bu = − 5 ~ + 5 mT, Bc = 0 ~ 60 mT, average time = 200 msec, average of four measurements) and cross sections (d) along horizontal line at Bu = 0.5 mT and (e) along vertical line at Bu = 31 mT.

Additional File 4: Figure S4. Results of analyses using MAX Unmix software (Maxbauer et al. 2016) for samples (a) MC10CB07-1 (bulk sample), (b) MC10CB07-2-S2-M-1 (magnetic extract after chemical leaching), and (c) MC10CB07-2-NM (material left after magnetic extract). Each diagram shows the distribution of coercivity spectrum with horizontal scale as logarithm of field B in mT and vertical scale as dM/dlog (B), where M represents magnetization in Am^2. Gray circles and orange curves represent raw data points and models as combination of the optimized magnetization components, respectively. Green, purple, blue, and red curves (shading as 95% error bands) are components 1, 2, 3, and 4, respectively. Simple log-normal distribution was used. Bh and DP are mean coercivity and dispersion parameter for each log-gaussian distribution, respectively. Uncertainty of each parameter is 1σ.

Abbreviations

AGM: alternating gradient magnetometer; EDS: energy-dispersive X-ray spectrometry; FE-SEM: field emission-scanning electron microscope; FORC: first-order reversal curve; IRM: isothermal remanent magnetization; SQUID: superconducting quantum interference device; XRD: X-ray diffraction; XRF: X-ray fluorescence.

Authors' contributions
Hirokuni Oda designed the rock magnetic experiment, interpreted and wrote most of the manuscript; Yoshio Nakasato conducted chemical leaching and observations with optical and electron microscopes and analyzed with XRD/EDS/XRF, Akira Usui conducted sampling and provided the description of the ferromanganese crust. All authors read and approved the final manuscript.

Author details
[1] Research Institute of Geology and Geoinformation, Geological Survey of Japan, AIST, Central 7, 1-1-1 Higashi, Tsukuba 305-8567, Japan. [2] Sumiko Resources Exploration & Development Co., Ltd., 8-21, 3-Chome, Toranomon, Minato-ku, Tokyo 105-0001, Japan. [3] Center for Advanced Marine Core Research, Kochi University, B200 Monobe, Nankoku, Kochi 783-8502, Japan.

Acknowledgements
The authors thank all the crew and shipboard participants of the SOPAC cruises within Micronesia sea area for supporting us during on-site sampling. HO thanks Ayako Katayama and Emiko Miyamura for producing the figures and a part of the measurements. HO appreciates general discussions held with Andrew Roberts, David Heslop, Xiang Zhao, Pengxiang Hu, Richard Harrison, and Adrian Muxworthy. The authors are grateful to the valuable suggestions given by the editor (John Tarduno) and the reviewers (Joshua Feinburg and an anonymous) for the manuscript.

Competing interests
The authors declare that they have no competing interests.

Availability of data and materials
Data will be available upon request to the authors.

Consent for publication
Not applicable.

Ethics approval and consent to participate
Not applicable.

Funding
This work is partially supported by funding from AIST/METI, Japan relating to "Development of machine learning approaches in magnetic recording and climate research" to HO.

Publisher's Note

Received: 2 August 2018 Accepted: 15 September 2018
Published online: 05 October 2018

References

Anthony JW, Bideaux RA, Bladh KW, Nichols MC (eds) (2018) Handbook of mineralogy. Mineralogical Society of America, Chantilly, VA, USA, pp 20151–1110. http://www.handbookofmineralogy.org/

Bazylinski D, Garratt-Reed A, Frankel R (1994) Electron microscopic studies of magnetosomes in magnetotactic bacteria. Microsc Res Tech 27:389–401. https://doi.org/10.1002/jemt.1070270505

Chang L, Roberts A, Winklhofer M, Heslop D, Dekkers M, Krijgsman W, Gerald J, Smith P (2014) Magnetic detection and characterization of biogenic magnetic minerals: A comparison of ferromagnetic resonance and first-order reversal curve diagrams. J Geophys Res Solid Earth 119:6136–6158

Egli R (2013) VARIFORC: An optimized protocol for calculating non-regular first-order reversal curve (FORC) diagrams. Glob Planet Change 110:302–320

Gleason JD, Moore TC, Rea DK, Johnson TM, Owen RM, Blum JD, Hovan SA, Jones CE (2002) Ichthyolith strontium isotope stratigraphy of a Neogene red clay sequence: calibrating eolian dust accumulation rates in the central North Pacific. Earth Planet Sci Lett 202(3):625–636

Harrison R, Feinberg J (2008) FORCinel: An improved algorithm for calculating first-order reversal curve distributions using locally weighted regression smoothing. Geochem Geophys Geosystems 9:Q05016. https://doi.org/10.1029/2008GC001987

Hein JR, Yeh HW, Gunn SH, Sliter WV, Benninger LM, Wang CH (1993) Two major Cenozoic episodes of phosphogenesis recorded in equatorial Pacific seamount deposits. Paleoceanography 8(2):293–311. https://doi.org/10.1016/lj.cageo.2016.07.009

Joshima M, Usui A (1998) Magnetostratigraphy of hydrogenetic manganese crusts from Northwestern Pacific seamounts. Marine Geology 146(1–4):53–62

Kim J, Hyeong K, Jung HS, Moon JW, Kim KH, & Lee I (2006) Southward shift of the Intertropical convergence zone in the western Pacific during the late tertiary: evidence from ferromanganese crusts on seamounts west of the Marshall Islands. Paleoceanography 21(4)

Kind J, Gehring A, Winklhofer M, Hirt A (2011) Combined use of magnetometry and spectroscopy for identifying magnetofossils in sediments. Geochem Geophys Geosystems 12:Q08008. https://doi.org/10.1029/2011GC003633

Koschinsky A, Halbach P (1995) Sequential leaching of marine ferromanganese precipitates: genetic implications. Geochim Cosmochim Acta 59(24):5113–5132

Lin W, Pan Y, Bazylinski D (2017) Diversity and ecology of and biomineralization by magnetotactic bacteria. Environ Microbiol Rep 9:345–356. https://doi.org/10.1111/1758-2229.12550

Lowrie W (1990) Identification of ferromagnetic minerals in a rock by coercivity and unblocking temperature properties. Geophys Res Lett 17:159–162. https://doi.org/10.1029/gl017i002p00159

Maxbauer DP, Feinberg JM, Fox DL (2016) MAX UnMix: A web application for unmixing magnetic coercivity data. Comput Geosci 95:140–145

Nishi K, Usui A, Nakasato Y, Yasuda H (2017) Formation age of the dual structure and environmental change recorded in hydrogenetic ferromanganese crusts from Northwest and Central Pacific seamounts. Ore Geol Rev 87:62–70. https://doi.org/10.1016/j.oregeorev.2016.09.004

Noguchi A, Yamamoto Y, Nishi K, Usui A, Oda H (2017a) Paleomagnetic study of ferromanganese crusts recovered from the northwest Pacific—Testing the applicability of the magnetostratigraphic method to estimate growth rate. Ore Geol Rev 87:16–24. https://doi.org/10.1016/j.oregeorev.2016.07.018

Noguchi A, Oda H, Yamamoto Y, Usui A, Sato M, Kawai J (2017b) Scanning SQUID microscopy of a ferromanganese crust from the northwestern Pacific: Sub-millimeter scale magnetostratigraphy as a new tool for age determination and mapping of environmental magnetic parameters. Geophys Res Lett 44(11):5360–5367. https://doi.org/10.1002/2017GL073201

Oda H, Usui A, Miyagi I, Joshima M, Weiss BP, Shantz C, Frong LE, Mcbride KK, Harder R, Baudenbacher FJ (2011) Ultrafine-scale magnetostratigraphy of marine ferromanganese crust. Geology 39(3):227–230

Oda H, Kawai J, Miyamoto M, Miyagi I, Sato M, Noguchi A, Yamamoto Y, Fujihira J, Natsuhara N, Aramaki Y, Masuda T, Xuan C (2016) Scanning SQUID microscope system for geological samples: system integration and initial evaluation. Earth Planets Space 68:179. https://doi.org/10.1186/s40623-016-0549-3

Roberts A, Heslop D, Zhao X, Pike C (2014) Understanding fine magnetic particle systems through use of first-order reversal curve diagrams. Rev Geophys 52:557–602

Tarduno JA (1990) Absolute inclination values from deep sea sediments: A reexamination of the Cretaceous Pacific record. Geophys Res Lett 17:101–104

Tarduno JA, Duncan RA, Scholl DW, Cottrell RD, Steinberger B, Thordarson T, Kerr BC, Neal CR, Frey FA, Torii M, Carvallo C (2003) The Emperor Seamounts: Southward motion of the Hawaiian hotspot plume in Earth's mantle. Science 301:1064–1069

Usui A, Graham IJ, Ditchburn RG, Zondervan A, Shibasaki H, Hishida H (2007) Growth history and formation environments of ferromanganese deposits on the Philippine Sea Plate, northwest Pacific Ocean. Isl Arc 16(3):420–430

van Hinsbergen D, Groot L, Schaik S et al (2015) A paleolatitude calculator for paleoclimate studies. PLoS ONE 10:e0126946. https://doi.org/10.1371/journal.pone.0126946

Yamagishi A, Tanaka M, Lenders J, Thiesbrummel J, Sommerdijk N, Matsunaga T, Arakaki A (2016) Control of magnetite nanocrystal morphology in magnetotactic bacteria by regulation of mms7 gene expression. Sci Rep 6:29785. https://doi.org/10.1038/srep29785

Yuan W, Zhou H, Zhao X, Yang Z, Yang Q, Zhu B (2017) Magnetic stratigraphic dating of marine hydrogenetic ferromanganese crusts. Sci Rep 7:16748